Influence of the thermal environment on entanglement dynamics in small rings of qubits

Nikola Burić*
Institute of Physics, University of Belgrade, PO Box 68, 11000 Belgrade, Serbia
(Received 30 October 2007; published 17 January 2008)

Numerical solutions of the stochastic Schrödinger equation given by quantum state diffusion approach to open quantum systems is used to study dynamics of nearest neighbor qubit pairs in systems of small number of qubits on rings with Heisenberg and transverse Ising interaction and under the influence of the thermal environment. In particular, the dependence of the pair entanglement dynamics on the temperature, number of qubits, the type of coupling, and the type of entanglement in the initial state was analyzed for systems of up to $N=10$ qubits. Periodic recurrence of relatively large values of the pair entanglement with dumping due to decoherence by the thermal noise is observed. It is concluded that the pair entanglement in rings with transverse Ising coupling and prepared in a separable initial state is the most resistant on the decoherence effects of the thermal noise, compared to the Heisenberg coupling or initial states with different types of entanglement.

DOI: 10.1103/PhysRevA.77.012321 PACS number(s): 03.67.Mn

I. INTRODUCTION

The possibility of using the entanglement as a resource for quantum computation and communication [1] in practice is effected by the environmental decoherence. Thus studies of creation and conservation of the entangled states in quantum systems in real conditions are of paramount importance. Systems such as chains of few, up to $N=10$, spin are now available for experimental studies, and the coupling between the spins can be observed [2]. In these experiments the environmental influence, its effect on the entanglement in dependence on the spin coupling, has to be well understood and can be studied. Such systems are commonly modeled by a collection of few coupled spins in interaction with a thermal bath of harmonic oscillators. Theoretical studies of these models can be quite involved because analytical solutions are usually not available and numerical solutions of the corresponding master equations are quite consuming.

Entanglement in spin chains has been extensively studied [3]. However, the major part of these studies concentrate on the static properties of the entanglement in the system's ground state or in the state of thermal equilibrium, and creation and dynamics of the entanglement in spin chains with the environmental influence has been studied much less. One of the first studies is reported in [4], where dynamics of two-site entanglement in the anisotropic XY model with periodic boundary condition and with no environmental effects was studied, using analytic results in the thermodynamic limit $N\rightarrow\infty$. In [5] a concept of entanglement flow in multiparticle systems was introduced and entanglement rate equations, which relate the rate of change of entanglement to already present entanglement, were suggested. Entanglement dynamics in systems with two or three qubits with or without decoherence was analyzed, for example, in [6,7]. Transport of entanglement in open-ended spin chains, and the possibility to use such chains as quantum wires, has been studied, and some recent references on this topic are, for example [8–11]. Entanglement dynamics in approaching and in the steady state in a system with nonconstant number of qubits and decoherence was studied in [12], using exact solutions for a pair of qubits with Ising Hamiltonian. Recently [13], entanglement dynamics in a small open chain of Josephson charge qubits, which is naturally written as a chain of coupled spins, with realistic disorder and noise, has been studied numerically, using time dependent density matrix renormalization group method [14] to approximate the state dynamics. In this paper, we considered small rings of up to $N=10$ spins with either Heisenberg or transverse Ising interaction weakly coupled to a thermal environment. Our main goal is to answer the following question: Which combination of the types of initial state and the types of coupling leads to the largest pair entanglement between the considered pair of qubits after some predetermined period of time? To that end, we have analyzed how the dynamics of the entanglement between nearest neighbors depends on (a) the number of spins in the ring, (b) temperature of the environment, (c) the type of the coupling among the spins, and (d) the entanglement of the initial state.

The study of entanglement dynamics in finite chains and the environmental influence is hampered by the fact that no analytic solutions of the relevant dissipative equations are available, and numerical solutions for the evolution of the state $\rho(t)$ require large storage space. Furthermore, it is not always clear what the relevant dynamical equations are when the Markov approximation cannot be applied.

In this paper, we shall assume that the thermal environment, its coupling to the system of few qubits, and the interspins coupling are such that the Markov approximation is valid, and we shall use numerical solutions of a particular stochastic unraveling of the Linblad master equation given by the quantum state diffusion theory (QSD) [15], to study the entanglement dynamics. The state space of the resulting stochastic Schrödinger equation (SSE) is 2^N times smaller than the dimension of the state space of the Linblad equation. Correlations between different components of the neighboring spins $\mathrm{Tr}[\rho\sigma_i^j\sigma_{i+1}^k]$; $i=1,\ldots,N$, j, $k=x,y,z$, which are needed to calculate the state ρ reduced over the ring except the considered pair of neighboring spins, are given as stochastic averages $E[\langle\sigma_i^j\sigma_{i+1}^k\rangle]$ over realizations of the stochas-

*buric@phy.bg.ac.yu

tic process. A number of sample paths taken to perform the averaging and the duration of the simulated evolution have been taken large enough to obtain definite understanding of the results.

The structure of the paper is as follows. In the next section we describe the considered rings of qubits and the type of the environmental influence, and then provide a short summary of the quantum state diffusion method that we used for numerical computations. Results of the numerical computations are presented and discussed in Sec. III, after a brief recapitulation of the definition of the entanglement of formation for bipartite systems of qubits, which we used as a measure of the nearest neighbor entanglement. Section IV contains a short summary and our main conclusions.

II. MODELS AND THE CALCULATION METHOD

Systems of qubits on a ring lattice with N sites and coupled via Heisenberg or transverse Ising interactions are described by the following Hamiltonians:

$$H = \sum_{i}^{N} \omega\sigma_i^z + J\sum_{i}^{N} (\sigma_i^x\sigma_{i+1}^x + \sigma_i^y\sigma_{i+1}^y + \sigma_i^z\sigma_{i+1}^z), \quad N+1=1 \tag{1}$$

or

$$H = \sum_{i}^{N} \omega\sigma_i^z + J\sum_{i}^{N} \sigma_i^x\sigma_{i+1}^x, \quad N+1=1. \tag{2}$$

where $\sigma_i^{x,y,z}$ are the three Pauli matrices of the ith qubit, J is the coupling strength, and ω corresponds to the frequency of precession around z axes of the state of a decoupled qubit. The crucial difference between Eqs. (1) and (2), which is clearly manifested in the entanglement dynamics [6], is that Eq. (1) is symmetric under rotations around z axes, and Eq. (2) has no such symmetry. We shall consider systems (1) and (2) in the geometric configuration of a ring, that is the boundary condition is given by $\sigma_{N+1}=\sigma_1$.

The Schrödinger-Liouville equation $\dot{\rho}=-i[H,\rho]$ with the Hamiltonians (1) or (2) describes the evolution of the system in complete isolation from the environment. In real systems there are environmental perturbations of different types, depending on the particular properties of the physical system modeled by the Hamiltonians of the type (1) or (2), and they crucially affect the dynamics of the entanglement. If the environment and the system satisfy the conditions of Markov approximation [16] then the most general completely positive continuous evolution of the open system is described by the Linblad master equation [17,16]

$$\frac{d\rho(t)}{dt} = -i[H,\rho] - \frac{1}{2}\sum_{k}[L_k\rho,L_k^\dagger] + [L_k,\rho L_k^\dagger], \tag{3}$$

where $-i[H,\rho]$ describes the unitary part and the rest is the dissipative part. The Hamiltonian H in Eq. (3) is in general different from the Hamiltonian that describes the isolated system, but under the assumed Markov property and for qubits with local environments, the difference is small and can be incorporated as a small correction of the parameters in the original Hamiltonian.

Linblad operators L_k describe all different types of the influence that the environment exerts on the system. Standard models of these influences, when the environment of each of the qubits can be considered independently of the environments of the other qubits, include the thermal environment, described by local Linblad operators $L_i \equiv \mathbf{1}_1 \otimes \ldots (L_i) \ldots \otimes \mathbf{1}_N$ where, for each qubit,

$$L_i = \frac{\Gamma(\bar{n}+1)}{2}\sigma_i^- + \frac{\Gamma\bar{n}}{2}\sigma_i^+. \tag{4}$$

The operators L_i induce dissipation [the first term in Eq. (4)] and excitation (the second term) processes between the two levels of each of the qubits. The parameter $\bar{n}$ is proportional to the temperature and Γ is treated here as a phenomenological parameter that describes the coupling of a qubit with its thermal environment [13,18]. Well known derivation (see for example [19]) of the Linblad master equation (3) and the form of the Linblad operators (4) that correspond to the thermal environment, starts with a Hamiltonian microscopic model of spins and a large collection of bosonic modes, which interact independently with each of the spins. The derivation is based on the perturbation expansion in the spin-boson coupling, and assumed properties of the bosonic modes, such as the Markov property and a very large number of the bosonic modes. These assumptions are valid if the microscopic model and its parameters satisfy certain properties. As a result, the master equation (3) and the Linblad operators (4) with the parameter *gamma* that explicitly depends on the correlation properties of the bosonic modes are obtained. Of course, many particular systems of interacting qubits with bosonic environment, especially in the domain of solid state physics, do not satisfy the assumptions and the constraints on the parameter values that justify the derivation of Eq. (3). There are many types of generalized master equations that do not assume the Markov property of the environment [20,16]. For example, the relevant master equation might be of the form (3) but with the Linblad operators that depend explicitly on time and the systems initial state [21]. Nevertheless, we shall consider the spin-boson systems such that Eqs. (3) and (4) represent a good approximation of the qubits part dynamics. Then, the parameters in Eqs. (3) and (4) have to satisfy certain conditions: The phenomenological parameter Γ should be small, corresponding to the weak coupling, and the time scale of the environment dynamics should be small compared to the systems dynamics time scale. We shall suppose that $\bar{n}$ and Γ are equal for all qubits and that J and Γ are small $J, \Gamma \ll \omega$, and analyze the dynamics for different values of $\bar{n} \leq \omega$. Under these assumptions we can use the master equation (3) with the Hamiltonian (1) or (2) and the Linblad operators (4) as a good approximation to study the effects of the thermal environment on the entanglement dynamics in the systems of qubits (1) or (2). Since an application of dynamical equations, which result from treating the environment perturbatively, like Eq. (3) or Eq. (6) based on Markov-Born approximation, to study the asymptotic $t \to \infty$ dynamics is questionable, we shall concen-

trate on the influence of noise during a finite and relatively short period of time. This period is determined by the periodic features of the entanglement dynamics in the isolated system.

Equation (3) describes coupled evolution of 2^{2N} matrix elements of the state ρ, which requires quite large memory space for the numerical computations. As is well known, there is a class of alternative but equivalent descriptions of an open Markov system dynamics given entirely in terms of pure states. The evolution equation in these formulations is a stochastic Schrödinger equation with the state space of dimension 2^N. In fact, the density matrix ρ can be written, in different but equivalent ways, as a convex combination of pure states. Each of these results in a stochastic differential equation for $|\psi(t)\rangle$ in the Hilbert space $\mathcal{H}$. Such SSE's are called stochastic unraveling [15,22,16] of the Linblad master equation for the reduced density matrix $\rho(t)$. There are many different forms of nonlinear and linear SSE that have been used in the context of open systems [24,23,16,15,22] or suggested as fundamental modifications of the Schrödinger equation [15,25–30]. They are all consistent with the requirement that the solutions of Eq. (3) and of SSE satisfy

$$\rho(t) = E[|\psi(t)\rangle\langle\psi(t)|], \tag{5}$$

where $E[|\psi(t)\rangle\langle\psi(t)|]$ is the expectation with respect to the distribution of the stochastic process $|\psi(t)\rangle$. The advantages of the description in terms of the pure states and SSE over the description by ρ are twofold. On the practical side, which is why we shall use it, the computations are much more efficient, as soon as the size of the Hilbert space is moderate or large [34]. On the theoretical side, the stochastic evolution of pure states provides valuable insight which cannot be inferred from the density matrix approach [31,32,15,16,33,6].

There are two main approaches to the unraveling of the Linblad master equation: The method of quantum state diffusion [15] and the relative state method [23,16], with specific advantages associated with each of the methods. The relative state method is usually used to describe the situations when the measurement is the dominant interaction with the environment. The method offers particular flexibility in that the master equation can be unraveled into different stochastic equations conditioned on the results of measurement. On the other hand, the correspondence between the QSD equations and the Linblad master equations is unique, and is not related to a particular measurement scheme, or the form of the Markov environment. The resulting SSE is always of the form of a complex diffusion process on the Hilbert space of pure states.

In our computations we shall use the unraveling of the master equation given by the quantum state diffusion equation. The equation is given by the following formula:

$$|d\psi\rangle = -iH|\psi\rangle dt + \left[\sum_k 2\langle L_k^\dagger\rangle L_k - L_k^\dagger L_k - \langle L_k^\dagger\rangle\langle L_k\rangle\right]|\psi(t)\rangle dt + \sum_l (L_k - \langle L_k\rangle)|\psi(t)\rangle dW_k, \tag{6}$$

where $\langle\ \rangle$ denotes the quantum expectation in the state $|\psi(t)\rangle$ and dW_k are independent increments (indexed by k) of complex Wiener c-number processes $W_k(t)$ and satisfy

$$E[dW_k] = E[dW_k dW_{k'}] = 0,$$

$$E[dW_l d\bar{W}_{k'}] = \delta_{k,k'} dt,$$

$$k = 1,2 \ldots m, \tag{7}$$

where $E[\cdot]$ denotes the expectation with respect to the probability distribution given by the (m-dimensional) process W, and $\bar{W}_k$ is the complex conjugate of W_k.

We have used the QSD equation (6) with the Hamiltonians of the form (1) or (2) and the Linblad operators corresponding to the local thermal environment (4). In our case there are N Linblad operators, one of the form (4) for each qubit, so $m=N$. A single realization of the stochastic process (6) is used to calculate, for example, $\langle\sigma_i^j\sigma_{i+1}^k\rangle$; $j,\ k=x,y,z$, and then averaging over many sample paths gives the correlation functions $E[\langle\sigma_i^j\sigma_{i+1}^k\rangle]=\mathrm{Tr}[\rho\sigma_i^j i\sigma_{i+1}^k]$ which are needed for the calculation of the entanglement measure. It turns out that the number of sample paths needed for satisfactory results is not large, as we shall comment on the next section. The details of the algorithm for numerical solutions of Eq. (6) are explained in [34].

III. TWO SITE ENTANGLEMENT DYNAMICS: RESULTS OF NUMERICAL COMPUTATIONS

The state of a system of qubits interacting with an environment is a mixed state described by the density matrix ρ. Such a state is termed separable if the density matrix ρ can be written as a convex combination of matrices in product form, that is if $\rho=\Sigma_k\lambda_k\rho_{1,k}\otimes\ldots\rho_{N,k}$, where $\rho_{i,k}$ is a density matrix in the space of the ith qubit. Otherwise, the state ρ is an entangled state. Entangled states occupy a major part of the systems state space, and different types of entanglement of such states can be defined. A general theory of multipartite entanglement is far from completed (see, for example [37,18]). We shall be interested in the entanglement between only two qubits in the ring, and furthermore only for the case of the nearest neighbor $(i,i+1)$ qubits. The correlations among the considered pair of qubits are described by the reduced density matrix $\rho_{i,i+1}=\mathrm{Tr}_{\bar{i},\bar{i+1}}[\rho]$ where $(\bar{i},\bar{i+1})$ denotes that the trace is taken over the Hilbert spaces of all the qubits except the considered pair (q_i,q_{i+1}). The pair of qubits is entangled with the qubits in the rest of the chain and with the environment. In our calculations the dynamical effect of the entanglement with the rest of the chain is treated exactly and the entanglement with the environment is approximated as a noise described by the Linblad operators.

In the case of qubits isolated from the environment, the system remains in the pure state and the entanglement of the considered pair of qubits with the rest of the chain can be measured by the Von Neuman entropy of $\rho_{i,i+1}$, by treating the qubit pair and the rest of the chain as the two components of a bipartite system. However, we shall not be interested in the entanglement of the pair with the rest of the chain, but in the entanglement among the two qubits of the $(i,i+1)$ pair

$[(i,i+1)$ entanglement]. In general, a measure of the degree of entanglement among the two qubits which are not in a pure state, called the entanglement of formation [35,36], is defined by minimization of the expression $\Sigma_k p_k S(|\psi_k\rangle\langle\psi_k|)$ where S is the Von Neuman entropy of the pure state $|\psi_k\rangle$, over all possible convex expansions of the state $\rho_{i,i+1} = \Sigma_k p_k \| \psi_k \rangle$ where vectors $|\psi_k\rangle$ form a basis of pure states in the two qubit Hilbert space. Few other measures of bipartite entanglement exist, but would give qualitatively the same results for the dynamics of the $(i,i+1)$ entanglement. For a pair of qubits the entanglement of formation can be calculated by simple algebraic procedure. First, a concurrence is calculated by the following formula

$$C(\rho_{i,i+1}) = \max\{0, \sqrt{\lambda}_1 - \sqrt{\lambda}_2 - \sqrt{\lambda}_3 - \sqrt{\lambda}_4\}, \tag{8}$$

where $\lambda_1 > \cdots \lambda_4$ are the eigenvalues of the matrix $\rho(\sigma_i^y \otimes \sigma_{i+1}^y)\bar{\rho}(\sigma_i^y \otimes \sigma_{i+1}^y)$, where $\bar{\rho}$ is the complex conjugate of ρ calculated in the standard bases. The entanglement of formation is then given via the function

$$h(x) = -x \log_2(1-x)\, x - (1-x)\log_2(1-x)$$

by the following formula

$$E(\rho_{i,i+1}) = h\left(\frac{1+\sqrt{1-C(\rho_{i,i+1})}}{2}\right). \tag{9}$$

The state $\rho_{i,i+1}$ of the two qubits can be represented in the bases

$$\{\mathbf{1}, \sigma_i^k \otimes \mathbf{1}, \mathbf{1} \otimes \sigma_{i+1}^l, \sigma_i^k \otimes \sigma_{i+1}^l\}, \tag{10}$$

where the expansion coefficients are the correlation functions

$$\mathrm{Tr}_{i,i+1}[\mathrm{Tr}_{\bar{i},\bar{i+1}}[\rho]\sigma_i^k \sigma_{i+1}^l] = E[\langle \sigma_i^k \sigma_{i+1}^l \rangle]. \tag{11}$$

Thus, in order to calculate the dynamics of the entanglement of formation, we have to compute the averages $E[\langle\psi(t)|\sigma_i^k\sigma_{i+1}^l|\psi(t)\rangle]$ over the stochastic evolution $|\psi(t)\rangle$.

Our main goal is to understand the dependence of the $(i,i+1)$-entanglement dynamics on the type of interqubit interaction, the size of the ring N, temperature of the environment $\bar{n}$, and the initial state. As the initial states we have considered pure N qubit states with three different distributions of entanglement: The separable states

$$|\mathrm{sep}\rangle \equiv \langle \rightarrow_1, \uparrow_2, \uparrow, \ldots, \uparrow_N \rangle, \tag{12}$$

the states with only one $(i,i+1)$-pair maximally entangled and the rest in product form

$$|\mathrm{max}\rangle \equiv [(|\uparrow_1, \downarrow_2\rangle + |\downarrow_1, \uparrow_2\rangle) \otimes \ |\downarrow_3, \ldots, \downarrow_N\rangle)]/\sqrt{2}, \tag{13}$$

and an example of a state with distributed entanglement

$$|W\rangle \equiv (|\uparrow_1, \downarrow_2, \downarrow_3 \ldots \downarrow_N\rangle + |\downarrow_1, \uparrow_2, \downarrow_3 \ldots \downarrow_N\rangle \ldots + |\downarrow_1, \downarrow_2 \ldots \uparrow_N\rangle)/\sqrt{N}. \tag{14}$$

We shall present the results of numerical computations of $E(\rho_{i,i+1}(t))$ for a few illustrative small values of the temperature dependent parameter $\bar{n}$: $\bar{n}=0.1(\sim 41$ mK); $n^- = 0.5(\sim 91$ mK); $\bar{n}=0.8(\sim 123$ mK); $\bar{n}=1(\sim 144$ mK), and for N up to 10 qubits. In the presented results the parameters

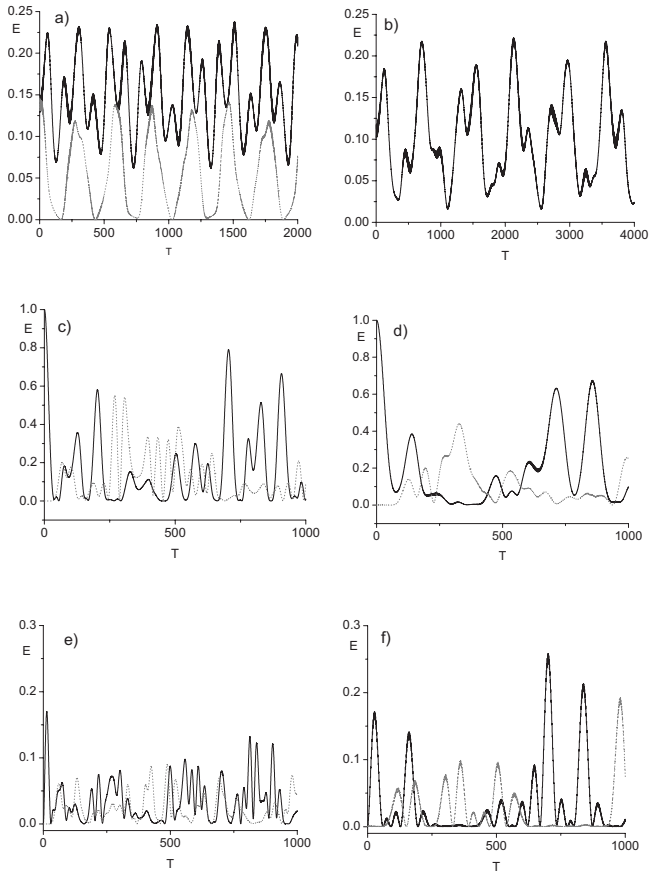

FIG. 1. $(1,2)$ (full black lines) and $(1+[N/2],2+[N/2])$ (dotted gray lines) pair entanglement for the isolated rings of qubits with Heisenberg (c), (e) and transversal Ising (a), (b), (d), (f) coupling. T represents the dimensionless time $T=\omega t$ and E is the measure of entanglement Eq. (9). In (a) and (b) the initial state is $|W\rangle$ and the number of qubits is (a) $N=7$ and (b) $N=8$. In (c) and (d) the initial state is $|\mathrm{max}\rangle$ and $N=7$. In (e) and (f) the initial state is $|\mathrm{sep}\rangle$ and $N=7$.

ω, the interqubit interaction J, and the coupling to the environment Γ are fixed $\omega=1$; $J=0.02$ and $\Gamma=0.02$ (compared with isolated system $\Gamma=0$). All time series are given in terms of the dimensionless time $T=t\omega$, and we use the units in which $\hbar=k=1$.

Isolated systems

Let us first describe the evolution of the $(i,i+1)$ entanglement for the isolated system, illustrated in Fig 1. These results serve a double purpose. They show what are the relevant time intervals for the $(i,i+1)$-entanglement dynamics, and indicate if the decrease of $(i,i+1)$ entanglement in the open system is mainly due to redistribution of the entanglement between the qubits or due to the decoherence by the environment. Figure 1 shows $(i,i+1)$ entanglement unitary dynamics given by Eqs. (1) and (2) starting from $|W\rangle$ and for $N=7,8$ [Figs. 1(a) and 1(b)] and from $|\mathrm{max}\rangle$ [Figs. 1(c) and 1(d)] and $|\mathrm{sep}\rangle$ [Figs. 1(e) and 1(f)] states for $N=7$. The isolated dynamics is similar for other numbers of qubits and is illustrated along with the entanglement dynamics with the

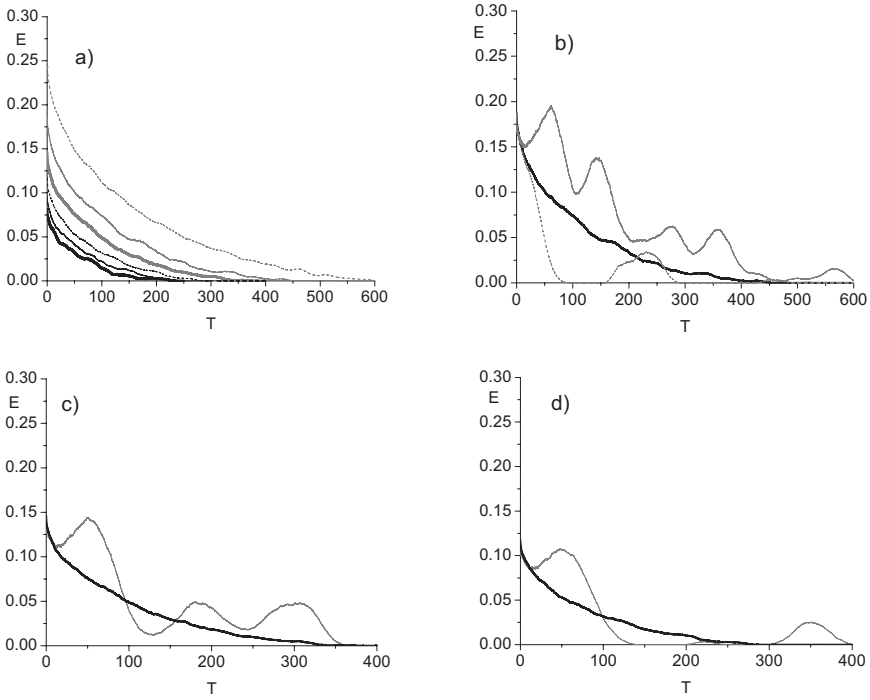

FIG. 2. Pair entanglement from $|W\rangle$ initial state and $\bar{n}=0.5$. (a) Heisenberg coupling and $N=5$ (dotted gray), $N=6$ (gray thin), $N=7$ (gray thick), $N=8$ (black dotted), $N=9$ (black thin), and $N=10$ (black thick). In (b), (c), and (d) the thick black lines are for the Heisenberg coupling, the full gray lines are for the transverse Ising (1, 2) pair and in (b) gray dotted for $(1+[N/2],2+[N/2])$ pair. (b) $N=6$; (c) $N=7$; (d) $N=8$. T and E are as in Fig. 1.

thermal noise (Figs. 2–6). Clearly, $E(t,|W\rangle)$ is a constant for the Heisenberg ring [Fig. 1(a)], and for the Ising case [Fig. 1(b)] it regularly oscillates around an average, which can depend on the position of the considered $(i,i+1)$ pair.

Dynamics from the initial state with maximally entangled pair is illustrated for $N=7$ in Fig. 1(c) for the Heisenberg and in Fig. 1(d) for the Ising cases. $(i,i+1)$ entanglement for the pairs $(1,2)$ and for $(4,5)$ are shown. Oscillations of the $(i,i+1)$ entanglement are irregular with some periodically recurring features. $(1,2)$ entanglement initially drops faster with the Hamiltonian (1) then with Eq. (2), then for a period of time it fluctuates with a relatively small amplitude, and then a few large oscillations (but smaller than the maximum) occur. This basic sequence keeps on repeating for ever. In the same time the entanglement of $(4,5)$ pair is created when $(1,2)$ drops, and in general large values of $(1,2)$ entanglement occur simultaneously with small values of $(4,5)$ entanglement and vice versa. Fluctuations in $(i,i+1)$ entanglement dynamics with the Hamiltonian (1) are faster than with the Hamiltonian (2). The basic period between the bursts of large values of entanglement among the fixed pair of qubits, denoted by τ_N, can be clearly identified in the case of the

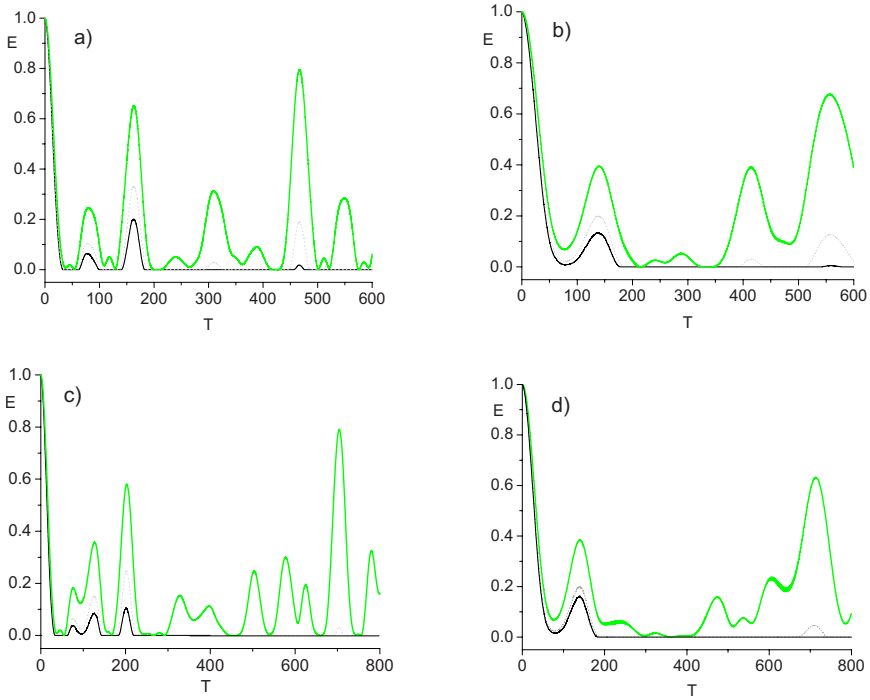

FIG. 3. (Color online) $(1,2)$ pair entanglement dynamics from $|\max\rangle$ initial state for (a) and (b) $N=6$ and (c) and (d) $N=7$, for the (a) and (c) the Heisenberg coupling and for (b) and (d) the transverse Ising. The parameter $\bar{n}$ is $\bar{n}=0.5$ (dotted gray), $\bar{n}=1$ (black), and isolated system (green). T and E are as in Fig. 1.

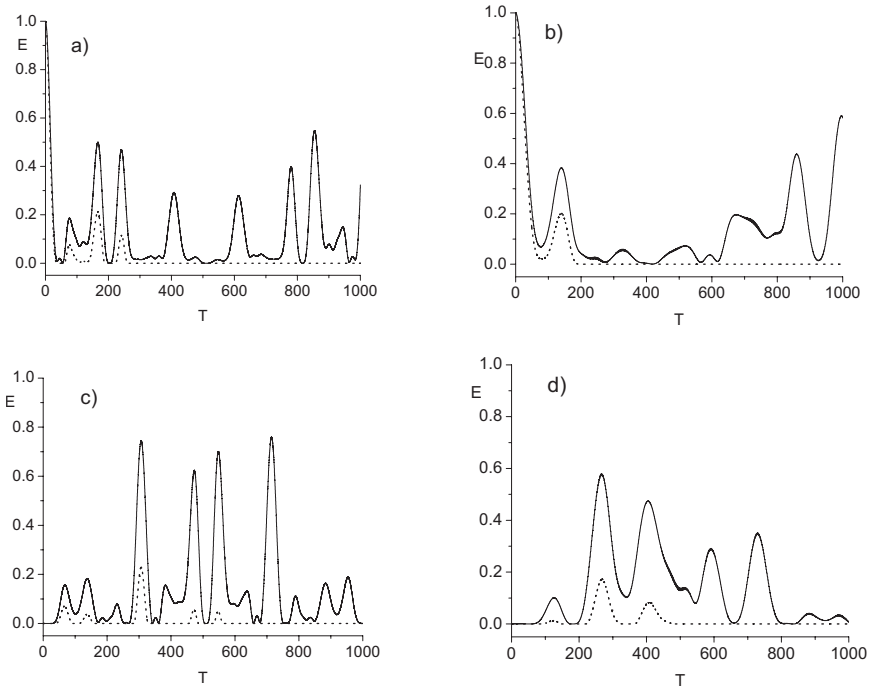

FIG. 4. (a) and (b) (1,2) and (c) and (d) (5,6) pair entanglement dynamics from $|\max\rangle$ initial state and $N=8$, for (a) and (c) the Heisenberg coupling and for (b) and (d) the transverse Ising, and $\bar{n}=0.5$ (black dotted) and isolated systems (black full). T and E are as in Fig. 1.

Ising coupling. In the analysis of the effects of the thermal environment we shall be interested in maximal temperatures such that the state of $(i,i+1)$ qubit is still entangled after this basic period τ_N.

The entanglement dynamics from a separable initial state strongly depend on the initial state. However, some qualitative features are independent of the initial state. The succession of few oscillations with relatively large amplitudes followed by a period of fluctuations with smaller amplitudes can be observed. The period between the bursts is roughly constant in time. In the case of Ising interaction [Fig. 1(f)] this is obvious, and is less clear in the Heisenberg case [Fig. 1(c)], since the difference between the peaks and smaller amplitude fluctuations is smaller. Nevertheless, similarly to the case of $|\max\rangle$ initial condition, the basic period τ_N can be defined using the Ising chain. Also large values of (1,2) entanglement are roughly simultaneous with small values of (4,5) entanglement. This is quite clear in the case of Ising interaction and in general is also true for the dynamics with the Heisenberg coupling.

We shall now discuss the $(i,i+1)$ entanglement dynamics under the influence of the thermal decoherence described by the Linblad equation (4). Creation of entanglement between a pair of qubits, its redistribution between the qubits in the

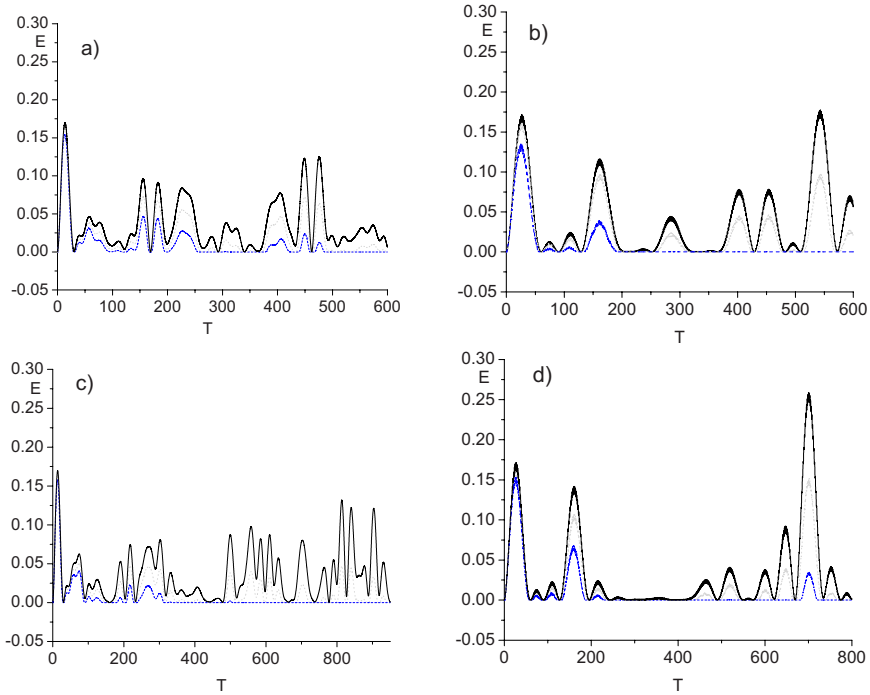

FIG. 5. (Color online) (1,2) pair entanglement dynamics from $|\mathrm{sep}\rangle$ initial state for (a) and (b) $N=6$ and (c) and (d) $N=7$, for (a) and (c) the Heisenberg coupling and for (b) and (d) the transverse Ising. In all figures $\bar{n}=0.5$ (dotted), $\bar{n}=0.8$ (dashed), and isolated system (full). T and E are as in Fig. 1.

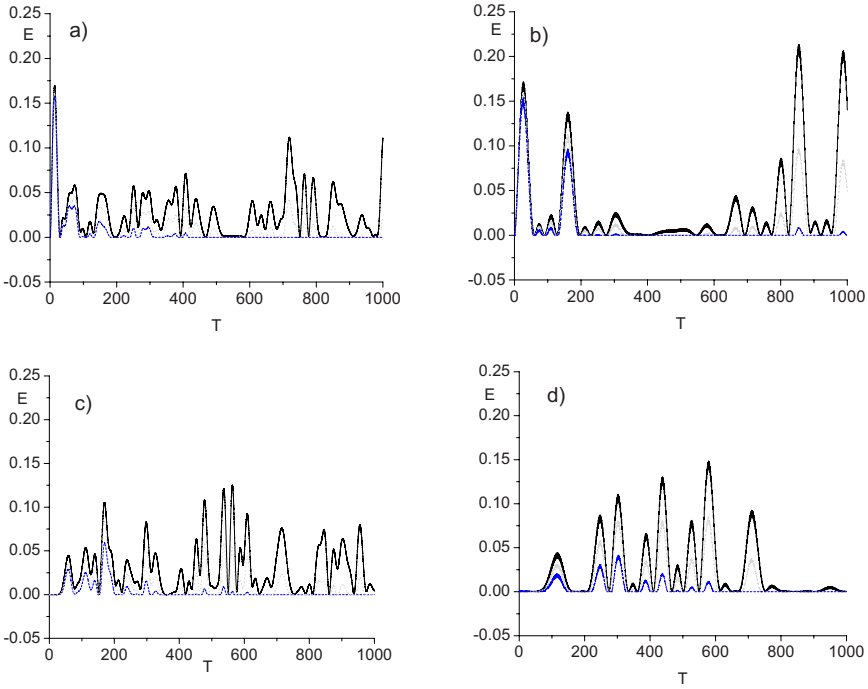

FIG. 6. (Color online) (a) and (b) (1,2) and (c) and (d) (5,6) pair entanglement dynamics from $|\text{sep}\rangle$ initial state for $N=8$, for (a) and (c) the Heisenberg coupling and for (b) and (d) the transverse Ising, and $\bar{n}=0.5$ (dotted), $\bar{n}=1$ (dashed), and isolated system (full). T and E are as in Fig. 1.

ring, and its loss due to the thermal noise act simultaneously to determine the nearest neighbor entanglement dynamics $E_{(i,i+1)}(t)$. The properties of the dynamics crucially depend on the type of the entanglement in the initial state, and also on the Hamiltonian, but the general features are qualitatively the same for rings with different N. Thus we shall present the results first for $|W\rangle$ initial states illustrated in Fig. 2, then for $|\text{max}\rangle$ initial states illustrated in Figs. 3 and 4 and finally for $|\text{sep}\rangle$ initial states (Figs. 5–7).

All computations of $E_{i,j}(t)$ that are illustrated in Figs. 2–7 have been done by averaging the solutions of the QSD equation (6) over only 200 sample paths. However, we have tested the computations using averaging over 100 and 1000 paths, and the results cannot be differentiated on the scale of the figures. Relatively small number of sample paths is needed to obtain the qualitatively clear results.

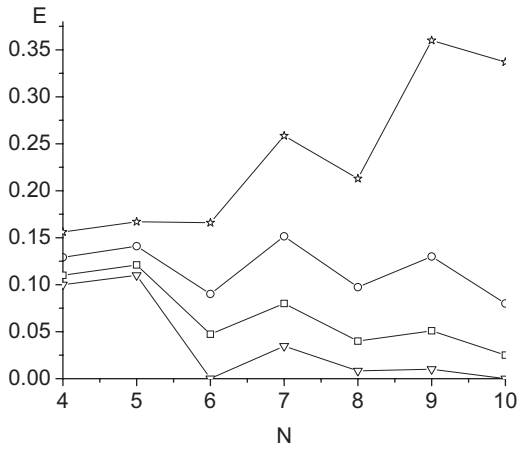

FIG. 7. Dependence of (1,2) pair entanglement E at $t=\tau_N$ on the number of qubits N for several fixed $\bar{n}$, for the transverse Ising coupling and $|\text{sep}\rangle$ initial state. (b) Isolated system (stars), $\bar{n}=0.5$ (circles), $\bar{n}=0.8$ (boxes), and $\bar{n}=1$ (down triangles). The lines serve only to guide the eye.

$|W\rangle$ initial states

Qualitative properties of $E_{(1,2)}(t)$ with $|W\rangle$ initial state are simple. For Heisenberg coupling $E_{(1,2)}(t)$ monotonically decreases to zero, and is equal for all $(i,i+1)$ pairs at all times. However, the decrease is more complicated than the simple exponential, since the rate of the decrease is not constant. In Fig. 2(a) we have illustrated $E_{(1,2)}(t)$ for $N=5,6,7,8,9,10$ and for $\bar{n}=0.5$. The decrease is, of course, slower for smaller $\bar{n}$, but $E_{(i,i+1)}(t)$ always goes to zero for some sufficiently large finite t. The dynamics of $E_{(i,i+1)}(t)$ with the Ising coupling (2), illustrated in Figs. 2(b)–2(d) for $N=6,7,8$, consists of relatively simple oscillations superimposed on the monotonic decrease. Again, $E_{(i,i+1)}(t)$ goes to zero for some sufficiently large finite t. The dynamics of $E_{(i,i+1)}(t)$ for different $(i,i+1)$ pairs can be different, and $E_{(i,i+1)}(t)$ with the Hamiltonian (2) can be larger or smaller than $E_{(i,i+1)}(t)$ with the Hamiltonian (1).

Let us now discuss the qualitative features of the pair entanglement dynamics from $|\text{max}\rangle$ and $|\text{sep}\rangle$ initial states. In the presentation of the results we shall use the following notation. By $E_{i,i+1}(t;|\psi_0\rangle,\bar{n})$ we shall denote the $(i,i+1)$ pair entanglement as a function of time when we want to refer to a specific initial state $|\psi_0\rangle$ and for some fixed $\bar{n}$. The symbol $E_{i,i+1}(t;|\psi_0\rangle,0)$ corresponds to the isolated system, i.e., $\Gamma=0$ and not to $\bar{n}=0$ in Eq. (4). If the dependence of a quantity like the period τ or $E_{i,j}$ on N wants to be stressed then we put N as a subindex of the corresponding quantity.

$|\text{max}\rangle$ initial states

The effect of the thermal noise on $E_{(i,i+1)}(t;|\text{max}\rangle,\bar{n})$ is to decrease the amplitudes of large oscillations and small fluc-

tuations that occur in the isolated system. In fact, the small fluctuations, between the times corresponding to the bursts of large peaks, completely disappear already for quite small $\bar{n}$. The relative decrease of large peaks increases in time. For temperatures larger than some $\bar{n}_0$, which depends on N, the entanglement wave, that is observed to go around the ring in the isolated systems, becomes overdumped and the maximal entanglement at $(i,i+1)$ pair of the initial state completely disappears before one period is completed. $\bar{n}_{0,N}$ increases proportionally with N, that is with the period of the entanglement wave, because the thermal noise acts locally on each of the qubits. For example, for the rings with either type of coupling and for $N=6$: n_0 is larger than 1; for $N=7$: n_0 is $0.5<n_0<0.8$; and for $N=8$: $n_0<0.5$. Comparison of $E_{(i,i+1)}\times(t;|\max\rangle,\bar{n})$ in rings with the different coupling and for different N and $\bar{n}$ shows that the relative decrease of pair entanglement during one period $E_{(i,i+1)}(t=\tau;|\max\rangle,\bar{n})/E_{(i,i+1)}(t=\tau;|\max\rangle,0)$ is always larger with the Heisenberg coupling. In the case of isolated rings we have seen that the pair entanglement after one period in the Heisenberg ring is larger than in the ring with the Ising coupling. Thus the initially maximal pair entanglement in the Ising case is faster distributed among qubits in the chain, but is also more robust with respect to the thermal noise, than with the Heisenberg coupling.

$|\mathrm{sep}\rangle$ initial states

The pair entanglement from an initially separable state $E_{i,i+1}(t;|\mathrm{sep}\rangle,\bar{n})$ survives decoherence by the thermal noise longer than from any of the other two types of initial states ($|W\rangle$ or $|\max\rangle$). $E_{1,2}(t;|\mathrm{sep}\rangle,\bar{n})$ are illustrated in Fig. 5, for $N=6,7$ and in Figs. 6(a) and 6(b) for $N=8$ together with $E_{5,6}(t;|\mathrm{sep}\rangle,\bar{n})$ [Figs. 6(c) and 6(d)]. The initial state is the separable state $|\mathrm{sep}\rangle$ given by Eq. (12). Values of $E_{i,i+1}(t;|\mathrm{sep}\rangle)$ depend on the initial state but the qualitative features are independent. As was pointed out, the temporal pattern of bursts of large peaks followed by periods of small amplitude fluctuations is clearly seen in the isolated system with the Ising coupling and survives the influence of small thermal noise. Also, the noise does not change the distribution of the periods of bursts and small values of $E_{i,i+1}$ in the ring. The period of time τ between the two successive bursts appears to be roughly constant in time. Thus, in the case of Ising coupling, we define the value of the parameter $\bar{n}=\bar{n}_0$, analogously as with the $|\max\rangle$ initial state, such that $E_{1,2}(t\geq\tau;|\mathrm{sep}\rangle,\bar{n})=0$ if $\bar{n}\geq\bar{n}_0$. The period τ depends on N at least for the type of initial separable states like $|\mathrm{sep}\rangle$, when all but one of the qubits are initially in the state $|\uparrow\rangle$. The pattern is much less clear in the rings with Heisenberg coupling. There are no peaks that exceed the average amplitude by more than double, and there are no clear long periods when $E_{i,i+1}(t;|\mathrm{sep}\rangle,\bar{n})$ is very small or zero. Nevertheless, for both types of the coupling we used τ as determined for the rings with the Ising coupling and the considered initial separable state, and we illustrate the dependence of the entanglement dynamics on $\bar{n}$ up to the time of the order of τ_N.

Like in the case of $|\max\rangle$ initial state, the main effects of the thermal noise, of dumping both the small oscillations and the large peaks, is the same in rings with either type of coupling. For small $\bar{n}$ and a short initial period of time $E_{1,2}(t;|\mathrm{sep}\rangle,\bar{n})$ is smaller than $E_{1,2}(t;|\max\rangle,\bar{n})$, but after some time the pair entanglement from the $|\mathrm{sep}\rangle$ becomes larger than that from the $|\max\rangle$. Thus, for example, at $\bar{n}_0$ corresponding to $|\max\rangle$ initial state $E_{1,2}(t\geq\tau;|\mathrm{sep}\rangle,\bar{n}_0)>E_{1,2}(t\geq\tau;|\max\rangle,\bar{n}_0)=0$. In other words, $\bar{n}_0$ for the separable initial state is clearly larger than with the $|\max\rangle$ initial state. This is true for all N that we have tested and for either type of the qubits coupling.

Comparison of peaks in the evolution of $E(t;|\mathrm{sep}\rangle,\bar{n})$ with different Hamiltonians and for the same $\bar{n}$ after similar periods of time shows that the large peaks of the pair entanglement generated by the transverse Ising dynamics are larger than the nearby large peaks generated by the Heisenberg Hamiltonian. This is true for all considered values of $\bar{n}$ and for all N. However, periods of small or zero values of the pair entanglement are, for small $\bar{n}$, longer in the Ising case.

In the following we shall concentrate on the case of the transverse Ising coupling, since the pair entanglement appears to be the most robust in this case. Dependence of $\bar{n}_0$ on the number of qubits N can be qualitatively inferred from Figs. 5 and 6 and similarly for other N. The dependence is indicated in Fig. 7 by plotting $E(t=\tau_N;|\mathrm{sep}\rangle,\bar{n})$ for different fixed $\bar{n}$. In the illustrated cases the recurrence period of large pair entanglement in the case of the Ising coupling is $\tau_6\simeq 550$, $\tau_7\simeq 700$, and $\tau_8\simeq 850$. Although the period τ increases with N, the pair entanglement after the period $E(t=\tau_{N+1};|\mathrm{sep}\rangle,\bar{n})$ for $N+1$ can be larger or smaller than $E(t=\tau_N;|\mathrm{sep}\rangle,\bar{n})$ for the same value of $\bar{n}$. Thus, for the same value of $\bar{n}$, the first peaks of $E_{1,2}(t;|\mathrm{sep}\rangle,\bar{n})$ for different N appear at the same time and have similar value, but at times of recurrence of the large peaks the values $E_{1,2}(t;|\mathrm{sep}\rangle,\bar{n})$ for different N differs. In fact, it seems that, at least for N up to $N=10$ that we have studied, $E_{1,2}(t;|\mathrm{sep}\rangle,\bar{n})$ for fixed $\bar{n}$, is smaller for $N=2k$ than for either $N=2k-1$ or $N=2k+1$. For example, for $\bar{n}=1$ the first maximum appears at $t\simeq 25$ independently of N. The values $E_{1,2}(t=25,|\mathrm{sep}\rangle,\bar{n})$ for different N are equal $E_{1,2}(t=25,|\mathrm{sep}\rangle,0)=0.17$ for isolated systems, and are similar for open system and small $\bar{n}$. However, at $\bar{n}=1$ and at times of first recurrence of the large value $E_{1,2}(t=\tau_N;|\mathrm{sep}\rangle,\bar{n})$ the (1,2) pair entanglement for the examples of $N=6,7,8$ are $E_{1,2}(t=\tau_6;|\mathrm{sep}\rangle,\bar{n})=0$, $E_{1,2}(t=\tau_7;|\mathrm{sep}\rangle,\bar{n})\simeq 0.035$, and $E_{1,2}(t=\tau_8;|\mathrm{sep}\rangle,\bar{n})\simeq 0.0088$. This is different from the case of $|\max\rangle$ initial state when $E(t=\tau_N,|\max\rangle,\bar{n})$ for the corresponding τ_N can only decrease with increasing N (or remain equal to zero), and consequently the corresponding $\bar{n}_0$ also decreases with N.

IV. SUMMARY

We have studied the time dependence of entanglement between the nearest neighbor qubits situated on a ring under the influence of the thermal environment. Rings with small number of qubits (up to $N=10$) in an external constant field and with Heisenberg or transverse Ising coupling have been analyzed. We were primarily interested in the dependence of

the pair entanglement dynamics on the number of qubits in the ring, the temperature of the environment, and the type of entanglement in the initial state, while other parameters, like the coupling strength between the qubits and between each of the qubits and the thermal environment, have been fixed to some typical constant value. The values of the parameters were in such a domain that the Markov approximation of the system-environment dynamics was justified. The entanglement dynamics from the initial states with distributed, localized, and zero entanglement has been studied. Time dependence of correlations between the pair of qubits have been calculated by numerical solutions of the corresponding quantum state diffusion equation, which is one of the methods that relies on stochastic representation in the Hilbert space of the system's pure states, and subsequent averaging over many sample pure state trajectories. The method of stochastic trajectories requires much smaller computer memory for computations, compared to the numerical solutions of the evolution equation in terms of the density matrix. We have demonstrated that the method can be used for efficient analyzes of the entanglement dynamics in the considered systems of qubits.

The dynamics of nearest neighbors entanglement for the pair of qubits initially in a separable or maximally entangled state shows a clear pattern of bursts of large values followed by a period when the entanglement is small. We have concentrated on the dynamics of the pair entanglement during the period of time up to the first recurrence of the burst of large values. Detailed comparison of the entanglement dynamics of the systems with Heisenberg and transverse Ising coupling, in particular the values of the pair entanglement after the characteristic period, for different temperatures, different number of qubits and different initial states, was performed. The most important differences between the entanglement dynamics with Heisenberg and transverse Ising coupling for different initial states can be summarized as follows. (a) In the case of $|W\rangle$ initial state and for the Heisenberg coupling the pair entanglement is monotonically decreasing and becomes zero for finite times. On the other hand, the entanglement dynamics with the transverse Ising coupling is that of oscillations superimposed on the monotonic decrease. This difference is easily understood since $|W\rangle$ state is invariant for the dynamics generated by the Heisenberg coupling and the local thermal noise does not introduce additional coupling of the qubits. (b) In the case of $|\max\rangle$ initial state the numerical calculations suggest the conclusion that the initially maximal pair entanglement in the Ising case is faster distributed among the qubits in the chain, but is more robust with respect to the thermal noise, than with the Heisenberg coupling. (c) Considering the pair entanglement dynamics from the separable $|\text{sep}\rangle$ initial state, we have concluded that the large peaks of the pair entanglement generated by the transverse Ising dynamics are larger than the nearby large peaks generated by the Heisenberg Hamiltonian. Furthermore, the dependence of the values at the peaks of the pair entanglement, after the characteristic period, on the number of qubits in the ring is more complicated in the case of transverse Ising coupling. Finally, the main conclusion of our numerical analysis is that the pair entanglement in the system with transverse Ising coupling initially prepared in the separable state is the most robust with respect to the decoherence by the thermal noise, compared with systems with Heisenberg coupling and/or entangled initial state. In the case of only two qubits, an explanation of the differences in the entanglement dynamics with Heisenberg or Ising coupling can be based on the abundance of entangled states and the restriction on the dynamics posed by the rotational symmetry in the Heisenberg case. The same symmetry argument provides a qualitative explanation of the observed differences of the entanglement dynamics in the case of small rings analyzed in this paper. Of course, the case of more than two qubits is much more difficult to understand in details because it involves a difficult question of the distribution of states with bipartite and multipartite entanglement.

In this paper, we have concentrated on the dependence of the entanglement dynamics on the temperature, number of qubits, initial state, and the type of coupling, but the interqubit coupling J was fixed to some small value. It would be interesting to investigate the role that the value of J plays in the entanglement dynamics with respect to the role played by the type of coupling and other parameters. For small variable values of J the analysis could be based on the Markov approximation of the environmental influence. Applicability of the Linblad master equations, or the equivalent QSD theory, is questionable for larger values of J when the time scale of the systems dynamics is shorter. Different types of noise, other than thermal considered here, might be important for different real systems. The qubits can interact via a nonlocal environment, and in this case the entanglement dynamics is quite different [38]. We have studied dynamics of the simplest type of entanglement that is possible in a multiqubit system. Still regarding only pairs of qubits, one could study the entanglement dynamics for pairs of separated qubits, and also investigate how the relation between the pair entanglement and the entanglement between the pair and the rest of the chain depends on the open system dynamics. Dynamics of multiparty entanglement should also be studied. Finally, we have chosen the Heisenberg and transverse Ising models, the type of the decoherence, and the domain of parameters with no regard to any similar experimentally available system, but in order to demonstrate that the QSD method is an efficient tool to study the entanglement dynamics in small rings of qubits. Similar numerical computations could be used to analyze the entanglement dynamics in particular experimentally available realizations of the qubits systems.

ACKNOWLEDGMENTS

This work is partly supported by the Serbian Ministry of Science Grant No. 141003. I should also like to acknowledge the support and hospitality of the Abdus Salam ICTP.

[1] M. A. Nielsen and I. L. Chuang, *Quantum Computation and Quantum Information* (Cambridge University Press, Cambridge, UK, 2001).
[2] C. F. Hirjibehedin *et al.*, Science **312**, 1021 (2006).
[3] L. Amico *et al.*, Rev. Mod. Phys. (to be published), e-print arXiv:quant-ph/0703044.
[4] L. Amico, A. Osterloh, F. Plastina, R. Fazio, and G. M. Palma, Phys. Rev. A **69**, 022304 (2004).
[5] T. S. Cubitt, F. Verstraete, and J. I. Cirac, Phys. Rev. A **71**, 052308 (2005).
[6] N. Buric, Phys. Rev. A **73**, 052111 (2006).
[7] K. Ann and G. Jaeger, e-print arXiv:quant-ph/0703216v1, 2007.
[8] V. Subrahmanyam, Phys. Rev. A **69**, 034304 (2004).
[9] S. F. Huelga and M. B. Plenio, Phys. Rev. Lett. **98**, 170601 (2007).
[10] A. Bayat and V. Karimipour, Phys. Rev. A **71**, 042330 (2005).
[11] A. Bayat and S. Bose, e-print arXiv:quant-ph/0706.4176v2.
[12] L. Hartmann, W. Dür, and H.-J. Briegel, Phys. Rev. A **74**, 052304 (2006).
[13] D. I. Tsomokos *et al.*, New J. Phys. **9**, 79 (2007).
[14] G. Vidal, Phys. Rev. Lett. **93**, 040502 (2004).
[15] I. C. Percival, *Quantum State Difussion* (Cambridge University Press, Cambridge, UK, 1999).
[16] H-P. Breuer and F. Petruccione, *The Theory of Open Quantum Systems* (Oxford University Press, Oxford, 2001).
[17] G. Lindblad, Commun. Math. Phys. **48**, 119 (1976).
[18] F. Mintert *et al.*, Phys. Rep. **415**, 207 (2005).
[19] C. Cohen-Tannoudji, J. Dupont-Roc, and G. Grynberg, *Atom-Photon Interactions* (Wiley, New York, 1992).
[20] U. Weiss, *Quantum Dissipative Systems* (World Scientific, Singapore, 1993).
[21] D. D. Bhaktavatsala Rao, V. Ravishankar, and V. Subrahmanyam, Phys. Rev. A **74**, 022301 (2006).
[22] V. P. Belavkin, Rep. Math. Phys. **43**, 405 (1999).
[23] H. J. Carmichael, *An Open Systems Approach to Quantum Optics* (Springer-Verlag, Berlin, 1983).
[24] C. W. Gardiner and P. Zoller, *Quantum Noise* (Springer-Verlag, Berlin, 2000).
[25] P. Pearle, Phys. Rev. A **48**, 913 (1993).
[26] A. Bassi and G. Chirardi, Phys. Rep. **379**, 257 (2003).
[27] N. Gisin, Helv. Phys. Acta **62**, 363 (1989).
[28] I. C. Percival, Proc. R. Soc. London, Ser. A **451**, 503 (1995).
[29] L. P. Hughston, Proc. R. Soc. London, Ser. A **452**, 953 (1996).
[30] S. L. Adler and T. A. Brun, J. Phys. A **34**, 4797 (2001).
[31] H. M. Wiseman and G. J. Milburn, Phys. Rev. A **47**, 642 (1993).
[32] K. Molmer, Y. Castin, and J. Dalibar, J. Opt. Soc. Am. B **10**, 524 (1993).
[33] N. Buric, Phys. Rev. A **72**, 042322 (2005).
[34] R. Schack, T. A. Brun, and I. C. Percival, Phys. Rev. A **53**, 2694 (1996).
[35] S. Hill and W. K. Wootters, Phys. Rev. Lett. **78**, 5022 (1997).
[36] W. K. Wootters, Phys. Rev. Lett. **80**, 2245 (1998).
[37] J. Eisert and D. Gross, e-print arXiv:quant-ph/0505149v2, 2006.
[38] F. Benatti, R. Floreanini, and M. Piani, Phys. Rev. Lett. **91**, 070402 (2003).